

# AZIMUTHAL DEPENDENCE OF THE MICROWAVE EMISSION FROM FOAM GENERATED BY BREAKING WAVES AT 18.7 AND 37 GHz

S. Padmanabhan, S. C. Reising

*Microwave Systems Laboratory, Electrical and Computer Eng. Dept., Colorado State University, Fort Collins, CO 80523*  
W. E. Asher

*Applied Physics Laboratory, Univ. of Washington Seattle, WA 98105*

L. A. Rose, P. W. Gaiser, J. P. Bobak, D. J. Dowgiallo and M. Anguelova  
*Naval Research Laboratory, Washington, DC 20375*

## ABSTRACT:

The need to improve retrieval of the surface wind vector and sea surface temperature (SST) from WindSat and the upcoming NPOESS Conical Microwave Imager Sounder (CMIS) motivated measurements of the microwave emission from breaking waves, both on the open ocean and in a wave basin. Aircraft and satellite measurements have demonstrated that the wind direction dependence of ocean surface brightness temperatures is small, on the order of 1-3 K peak-to-peak. Therefore, the accuracy of wind vector retrieval depends strongly upon quantitative knowledge of the relationship of the ocean surface emissivity to surface properties, such as sea surface wave spectrum and wave breaking. The effects of the surface wave spectrum have been addressed by many studies, but the azimuthal dependence of the microwave emission from breaking waves and foam has not been adequately addressed. Recently, a number of experiments have been conducted to quantify the increase in sea surface microwave emission due to foam. The Polarimetric Observations of the Emissivity of Whitecaps Experiment (POEWEX'04) was conducted during November 2004 to measure the azimuthal dependence of reproducible breaking waves in order to improve wind vector retrieval from spaceborne radiometric measurements, especially at wind speeds of 7 m/s and higher. The emissivity of breaking waves was shown to vary as a function of azimuth angle at four different WindSat frequencies.

## INTRODUCTION:

WindSat, the first polarimetric microwave radiometer on orbit, was launched in January 2003 to demonstrate retrieval of the full sea surface wind vector using passive microwave remote sensing. The National Polar-orbiting Operational Environmental Satellite System (NPOESS) Conical Microwave Imager/Sounder (CMIS), planned for first launch in 2010, is designed to retrieve the ocean surface wind vector as one of its six key environmental data records. Aircraft and satellite measurements have shown that the wind direction dependence of brightness temperatures at 10, 19 and 37 GHz is small, typically less than 3K peak-to-peak [1-4].

The NPOESS Integrated Operational Requirements Document requires a performance of  $\pm 20^\circ$  better in wind direction during 3 to 25-m/s winds at 20 km spatial resolution [1]. These requirements necessitate the quantification and removal of geophysical uncertainties in sea surface emission to an accuracy of approximately 0.1-0.2 K for horizontal polarization and 0.05-0.1 K for vertical polarization, both at 19 and 37 GHz. To date, some two-scale models have characterized the increase in microwave emission with wind speed as an aggregate effect of both surface roughness and foam [5]. However, foam substantially increases ocean microwave emission [6] with a wind speed dependence that changes in different wind speed regimes, so to achieve the accuracies needed for wind direction retrievals, microwave emission from foam needs to be characterized separately. To this end, the azimuth angle dependence of the microwave emission from foam needs to be quantified through carefully controlled experiments.

## PREVIOUS MEASUREMENTS:

Open ocean measurements have shown that emission due to foam depends on the incidence and/or azimuth angles of observation [7-8]. The intermittency of breaking waves on the open ocean makes it difficult to acquire reproducible measurements of beam-filling foam. Measurements as a function of incidence and azimuth angle under reproducible conditions are necessary to form useful conclusions about the look-angle dependence of emission due to breaking waves.

The Polarimetric Observations of the Emissivity of Whitecaps Experiment was conducted during 2002 at the OHMSETT wave basin in Leonardo, New Jersey [8]. The POEWEX'02 measurements showed that the increase in emission from a foam-free to a foam-covered water surface varies as a function of azimuth angle. Coordinated *in-situ* measurements demonstrated that the fundamental characteristics of waves in the wave tank are similar to those on the open ocean [8]. The increase in brightness temperatures due to breaking waves and foam was used to predict the increase in emission measured by a satellite radiometer which was significant for wind direction retrieval at wind speeds greater than 5 m/s.



**Figure 1. Microwave radiometers observing a breaking wave at the WindSat imaging frequencies (6.8, 10.8, 18.7 and 37 GHz) at the OHMSETT wave basin during the POEWEX'04 experiment.**

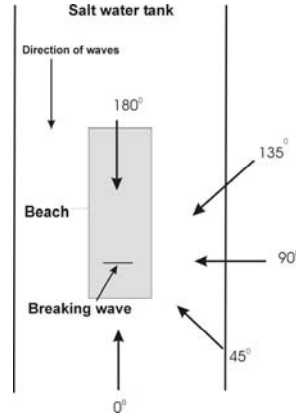


**Figure 2. The five azimuthal viewing directions of the radiometers.**

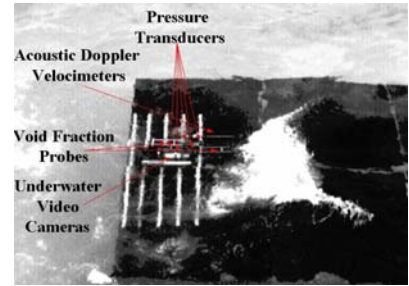


**Figure 3. *In-situ* instruments during POEWEX'04.**

**POEWEX'04:**

The POEWEX'02 measurements demonstrated that, in addition to the radiometric brightness temperature and foam fraction in the field of view, a number of additional physical parameters are required to obtain an accurate quantitative estimate of the azimuthal variation of the microwave emission from foam generated by breaking waves. Measurements of the wave slope spectrum during wave breaking are required to characterize accurately the effects of the instantaneous wave field and sea state on the increase in emission between a foam-free rough water surface and a foam-covered rough water surface. In addition, analysis of radiometric time series from the POEWEX'02 experiment showed that it is important to measure the foam-free rough water with no breaking waves in the field of view.

To provide these additional measurements and to characterize accurately the azimuthal dependence of breaking wave emission, the Polarimetric Observations of the Emissivity of Whitecaps Experiment (POEWEX'04) was conducted at the OHMSETT wave basin in Nov. 2004. Fig. 1 shows microwave radiometers at 6.8, 10.7, 18.7 and 37 GHz suspended below the basket of a boom-lift crane to measure microwave emission from breaking waves in the wave tank. The radiometers were positioned to view the water surface at azimuth angles of 0°, 45°, 90°, 135° and 180°, as defined in Fig. 2. At each azimuth angle, measurements were performed at incidence angles of 45°, 53° and 65°. The fractional area foam coverages in the fields of view of the radiometers were found by analyzing the bore-sighted video measurements using the grayscale

method of Asher and Wanninkhof [9]. This quantity is the fraction of pixels in the field of view of the radiometer whose value exceeds the brightness threshold distinguishing the breaking wave from the water background. The resulting fractional area foam coverage may include both actively breaking crests and decaying bubble plumes, and is called the foam fraction for brevity. Fig. 3 shows the configuration of the *in-situ* instruments with respect to the location of wave breaking. These *in-situ* instruments included pressure transducers, void fraction meters, underwater cameras and acoustic Doppler velocimeters. New measurements performed during POEWEX'04 include horizontally and vertically polarized brightness temperatures at 6.8 GHz, roughened surface emission with no breaking waves in the field of view and foam thickness. In addition, a new 2-D array of pressure transducers was deployed to measure the instantaneous wave field in the radiometers' fields of view. Fig. 4 shows the positions of the pressure transducers with respect to the breaking wave.

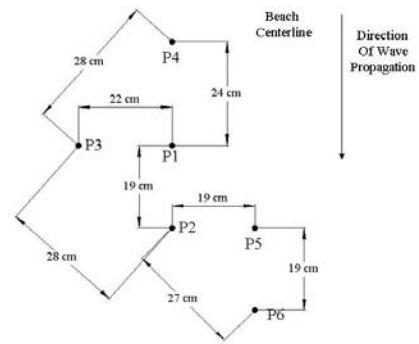


**Figure 4. The arrangement of pressure transducers in the OHMSETT wave tank during POEWEX'04.**

To calibrate the radiometers, tipping curves, liquid nitrogen and ambient microwave absorber measurements were performed before and after each azimuth angle measurement. The K- and Ka-band radiometers also performed internal calibrations every 45 seconds to correct for possible short-term gain variations. The antenna temperatures measured by the radiometers viewing the breaking wave and viewing the foam-free rough water (no breaking wave), along with the measured foam fraction, were used to calculate the emissivity of foam generated by breaking waves.

**RESULTS:**

Figs. 5 and 6 show the emissivity of foam for horizontal and vertical polarizations, respectively, at 18.7 GHz (red) and 37 GHz (black). A larger variation with azimuth angle was observed for horizontal than for vertical polarization, at both 18.7 GHz and 37 GHz.

The solid (horizontal polarization) and dotted (vertical polarization) curves in Fig. 7 show the azimuthally-averaged surface emissivity increases from a foam-free water surface to a foam-covered water surface at all frequencies. The triangles and circles represent the maximum and minimum increases in emissivity for the five azimuth angles measured. These results demonstrate that the azimuthal variation is a significant fraction of the mean emissivity increase at all four frequencies. In addition, it was observed that the mean and azimuthal variations of the increases in the emissivity vary with frequency. For the increases in emissivity measured at 6.8, 10.7, 18.7 and 37 GHz, the azimuthal variations as a percentage of the mean vary from 27.6% to 54% for vertical polarization and from 30.1% to 68.3% for horizontal polarization.

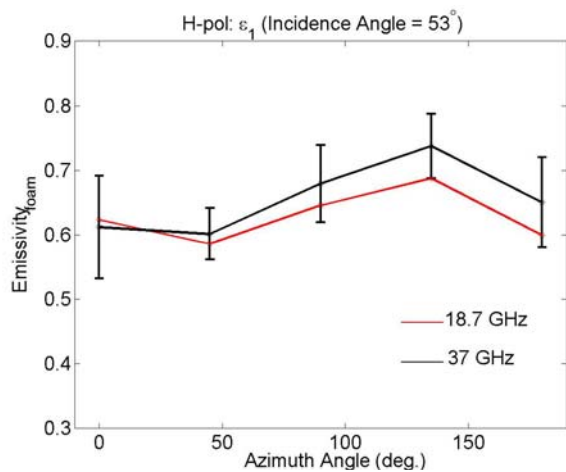


**Figure 5. Measured emissivity of foam for horizontal polarization at 53° incidence angle, at both 18.7 and 37 GHz.**

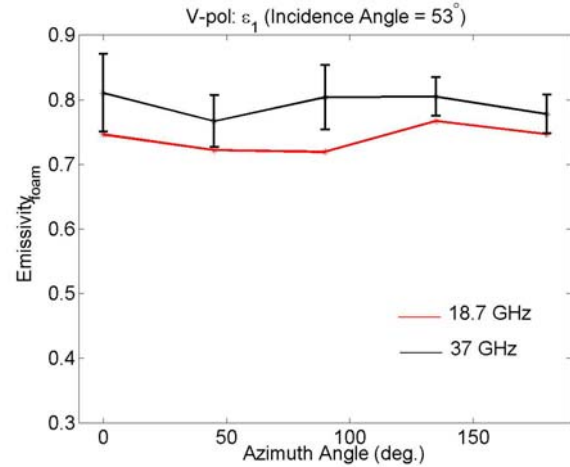


**Figure 6. Measured emissivity of foam for vertical polarization at 53° incidence angle, at both 18.7 and 37 GHz.**

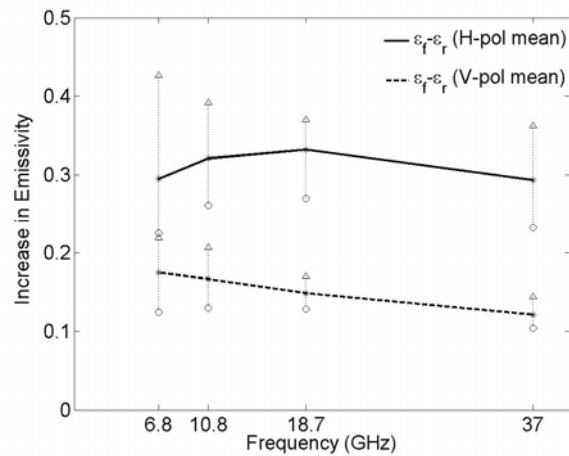


**Figure 7. Mean and azimuthal variation of increase in emissivity as a function of frequency at 53° incidence angle.**

Pressure transducer power spectra (Fig. 8) show that the large-scale wave field in the wave tank was consistent during all azimuth angle measurements at 53° incidence angle. The average video brightness of the area sampled by the void probe at 10 cm depth peaks ~1 sec before the peak measured by the void probe, as shown in Fig. 9. In addition, the void fraction enhancement is significantly shorter in duration than the video brightness enhancement. Therefore, an increase in optical brightness due to foam must be principally due to foam on the surface and not to subsurface bubbles.

The data points in Fig. 10 show the whitecap coverage measured on the open ocean as a function of wind speed during three experiments in three different geographic areas [10]. The empirical fit of these points to the Monahan and Lu model [11], also in Fig. 10, shows

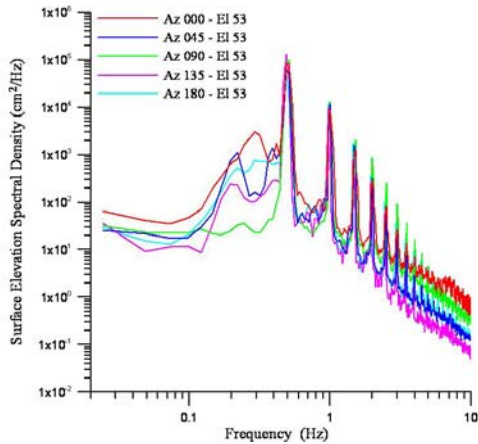


**Figure 8. Variability of wave height power spectra measured by a pressure transducer.**

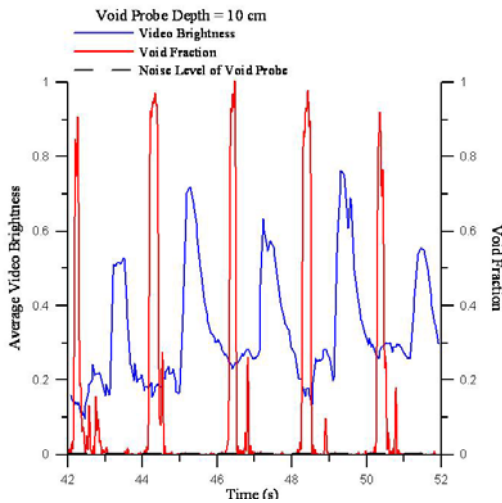


**Figure 9. Surface elevation spectral density measured by the pressure transducers.**

good agreement with measurements from WISE-2000 in the Mediterranean Sea [12]. Four different parameterizations including Asher et al. [10], Camps et al. [12] and two from Stramska and Petelski [13] were combined with the azimuthal averages of the increases in emissivities measured during POEWEX'04 to predict increases in brightness temperatures measured by a satellite radiometer. Figs. 11-14 show the increases in brightness temperature as a function of wind speed measured for horizontal and vertical polarizations at 18.7 and 37 GHz for four different wind speed parameterizations and an independent estimate from Wilheit's model [14]. At a wind speed of 15 m/s, the Stramska and Petelski models predict a 5 K and 2.5 K increase measured by a spaceborne radiometer at 18.7 GHz viewing a breaking wave at horizontal and vertical polarization, respectively. At 37 GHz the same models

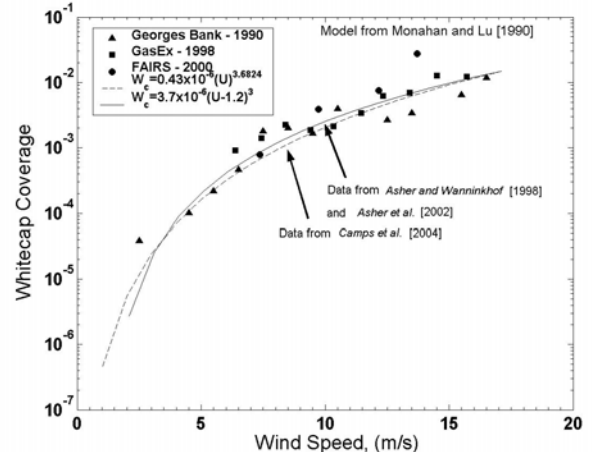


**Figure 10. Sea surface coverage by actively breaking waves for low to moderate wind speeds.**

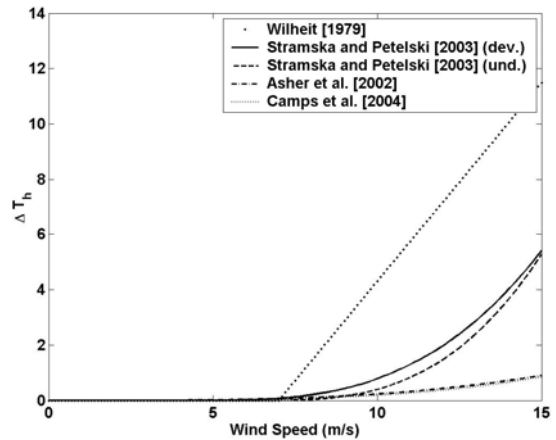


**Figure 11. Predicted increases in satellite brightness temperatures for horizontal polarization at 18.7 GHz using parameterizations of foam coverage.**

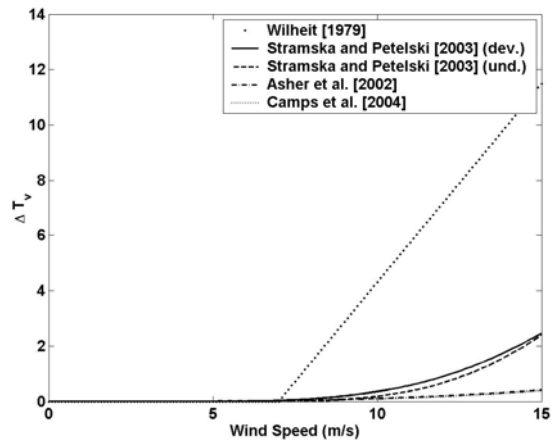


**Figure 12. Predicted increases in satellite brightness temperatures for vertical polarization at 18.7 GHz using parameterizations of foam coverage.**

predict an increase of 3.5 K and 1.5 K measured at horizontal and vertical polarization respectively. The estimated increases in brightness temperatures are significant at wind speeds greater than 7 m/s.

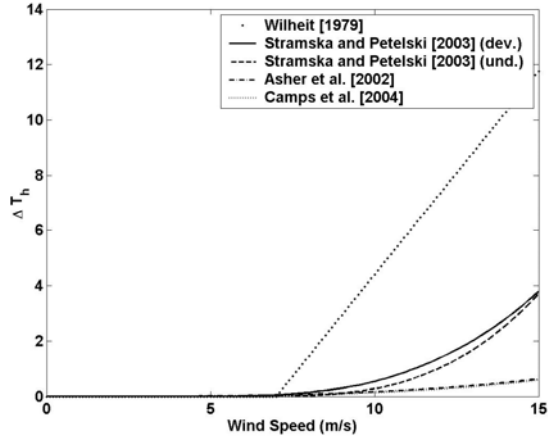


**Figure 13. Predicted increases in satellite brightness temperatures for horizontal polarization at 37 GHz using parameterizations of foam coverage.**

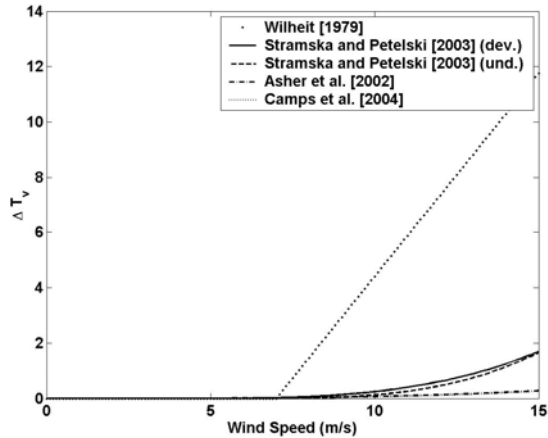


**Figure 14. Predicted increases in satellite brightness temperatures for vertical polarization at 37 GHz using parameterizations of foam coverage.**

### MODELING FOAM PERMITTIVITY:

The first step toward modeling sea foam emissivity at K and Ka-band is to calculate the effective dielectric permittivity of foam. For K-band and Ka-band, with  $\lambda_0 = 1.6$  cm and 0.8 cm respectively, one needs to consider the effects of both the multipole mechanism and the dipole approximation because for large bubbles with diameters 0.1-0.2 cm, both Rayleigh and Mie scattering need to be taken into account [15]. The dipole interaction of the bubbles is defined by the well known Lorentz-Lorentz

equation whereas the multipole mechanism is described by the Van De Hulst equations.

The Lorentz-Lorentz equation for dipole interaction is

$$\varepsilon_{N\alpha} = \frac{1 + \frac{8}{3} \pi N \overline{\alpha}}{1 - \frac{4}{3} \pi N \overline{\alpha}}$$

where

$$\overline{N\alpha} = \frac{k \int \alpha(a) f(a) da}{\frac{4}{3} \pi \int a^3 f(a) da} \quad \text{and}$$

$$\alpha = a^3 \frac{(\varepsilon_0 - 1)(2\varepsilon_0 - 1)(1 - q^3)}{(\varepsilon_0 + 2)(2\varepsilon_0 + 1)(1 - q^3) + 9\varepsilon_0 q^3}$$

The Van de Hulst equation describes the multipole-moment contribution of the bubbles as

$$\varepsilon_{NS} = 1 + i4\pi \left( \frac{2\pi}{\lambda} \right)^{-3} \overline{NS_0}$$

where

$$\overline{NS_0} = \frac{k \int S_0(a) f(a) da}{\frac{4}{3} \pi \int a^3 f(a) da} \quad \text{and}$$

$$S_0 = \sum_{n=1}^{\infty} \frac{2n+1}{2} (a_n + b_n)$$

$a$  is the external radius of a single bubble;

$f(a)$  is the normalized size-distribution function, which is assumed to be  $\gamma$ -distributed [16,17]:

$$f(a) = \frac{A^{B+1}}{\Gamma(B+1)} a^B e^{-Aa}$$

where  $A$  and  $B$  are parameters of the distribution, and  $A/B$  is the most probable radius [18];

$k$  is the packing coefficient of the bubbles;

$N$  is the volume concentration of the bubbles;

$\alpha$  is the complex polarizability of a single bubble;

$q = 1 - \delta/a$  is the bubble filling factor;

$\delta$  is the thickness of the shell;

$\varepsilon_0$  is the complex permittivity of the shell (usually salt water);

and  $a_n$  and  $b_n$  are the complex Mie coefficients for a hollow spherical particle.

Values of  $k$ ,  $N$ ,  $q$ ,  $f(a)$  measured during POEWEX'04 can be used to compute the dipole- and multipole-moment contributions to the effective permittivity of foam, which can then be used to calculate the Fresnel coefficients [18].

## CONCLUSIONS:

Breaking waves and foam significantly increase the upwelling microwave emission from the ocean surface. Since the ocean surface wind direction signature is small (~2-3 K), it is important to characterize the azimuthal dependence of the microwave emission of foam and to infer its contribution to the surface emission, separately from the effects of the sea surface spectrum.

POEWEX'04 was conducted to measure the azimuthal dependence of reproducible breaking waves to improve wind vector and SST retrieval from spaceborne radiometric measurements, especially at wind speeds of at least 7 m/s. The emissivity increases at 6.8, 10.7, 18.7 and 37 GHz are larger for horizontal polarization than for vertical, and the azimuthal variations are a significant percentage of the mean. These azimuthal variations are also more significant for horizontal polarization than for vertical.

The *in-situ* measurements during POEWEX'04 can be used to develop sea foam emissivity models at K and Ka-bands by calculating the absorption and scattering from the densely packed foam formed from breaking waves.

## ACKNOWLEDGMENTS

The National Polar-orbiting Operational Environmental Satellite System Integrated Program Office supported the Naval Research Laboratory's participation through Award NA02AANEG0338 and supported Colorado State University and the University of Washington through Award NA05AANEG0153.

## REFERENCES:

- [1] P.W. Gaiser, K.M. St. Germain, E.M. Twarog, G.A. Poe, W. Purdy, D. Richardson, W. Grossman, W.L. Jones, D. Spencer, G. Golba, J. Cleveland, L. Choy, R.M. Bevilacqua, and P.S. Chang, "The WindSat spaceborne polarimetric microwave radiometer: Sensor description and early orbit performance," *IEEE Trans. Geosci. Remote Sensing*, vol. 42, no. 11, pp. 2347-2361, Nov. 2004.
- [2] S. Yueh, W.J. Wilson, F.K. Li, W. Ricketts, and S.V. Nghiem, "Polarimetric microwave brightness signatures of ocean wind directions," *IEEE Trans. Geosci. Remote Sensing*, vol. 37, no. 2, pp. 949-959, Mar. 1999.
- [3] J.R. Piepmeier and A.J. Gasiewski, "High-resolution passive polarimetric microwave mapping of ocean surface wind vector fields," *IEEE Trans. Geosci. Remote Sensing*, vol. 39, no. 3, pp. 606-622, Mar. 2001.
- [4] G.A. Wick, J.J. Bates, and C.C. Gottschall, "Observational evidence of a wind direction signal in SSM/I passive microwave data," *IEEE Trans. Geosci. Remote Sensing*, vol. 38, no. 2, pp. 823-837, Mar. 2000.
- [5] F.J. Wentz, "A well calibrated ocean algorithm for SSM/I," *J. Geophys. Res.*, vol. 102, no. C4, pp. 8703-8718, Apr. 1997.
- [6] L.A. Rose, W.E. Asher, S.C. Reising, P.W. Gaiser, K.M. St. Germain, D.J. Dowgiallo, K.A. Horgan, G. Farquharson, and E.J. Knapp, "Radiometric measurements of the microwave emissivity of foam," *IEEE Trans. Geosci. Remote Sensing*, vol. 40, no. 12, pp. 2619-2625, Dec. 2002.
- [7] M.A. Aziz, S.C. Reising, W. E. Asher, L.A. Rose, P.W. Gaiser and K.A. Horgan, "Effects of air-sea interaction parameters on ocean surface microwave emission at 10 and 37 GHz," *IEEE Trans. Geosci. Remote Sensing*, vol. 43, no. 8, pp. 1763-1774, Aug. 2005.
- [8] S. Padmanabhan, S.C. Reising, W.E. Asher, L.A. Rose and P.W. Gaiser, "Effects of Foam on Ocean Surface Microwave Emission Inferred from Radiometric Observations of Reproducible Breaking Waves," *IEEE Trans. Geosci. Remote Sensing*, vol. 44, no. 3, pp. 569-583, Mar. 2006.
- [9] W.E. Asher and R. Wanninkhof, "The effect of bubble mediated gas transfer on purposeful dual gaseous experiments," *J. Geophys. Res.*, vol. 103, no. 10, pp. 555-560, May 1998.
- [10] W.E. Asher, J.B. Edison, W.R. McGillis, R. Wanninkhof, D.T. Ho, and T. Litchendorf, "Fractional area whitecap coverage and air-sea gas transfer during GasEx-98, in *Gas Transfer at Water Surfaces*, Geophys. Monogr. Ser., vol 127, M. A. Donelan et al., Ed. Washington, D.C.: AGU, 2002, pp. 199-204.
- [11] E.C. Monahan and M. Lu, "Acoustically relevant bubble assemblages and their dependence on meteorological parameters," *IEEE J. Ocean. Eng.*, vol. 15, no. 4, pp. 340-349, Oct. 1990.
- [12] A. Camps, J. Font, M. Vall-Illussera, C. Gabarro, I. Corbella, N. Duffo, F. Torres, S. Blamch, A. Aguias, R. Villarino, L. Enrique, J. J. Miranda, J. J. Arenas, A. Julia, J. Etcheto, V. Caselles, A. Weil, J. Boutin, S. Contardo, R. Niclos, R. Rivas, S. C. Reising, P. Wursteisen, M. Berger, M. Martin-Neira, "The WISE 2000 and 2001 field experiments in support of the SMOS mission: sea surface L-band brightness temperature observations and their application to sea surface salinity retrieval," *IEEE Trans. Geosci. Remote Sensing*, vol. 42, no. 4, pp. 804-823, Apr. 2004.
- [13] M. Stramska and T. Petelski, "Observations of oceanic whitecaps in the north polar waters of the Atlantic," *J. Geophys. Res.*, vol 108, no. C3, 31-1 – 31-10, 2003.
- [14] T. Wilhelm, "A model for the microwave emissivity of the ocean's surface as a function of wind speed," *IEEE Trans. Geosci. Remote Sensing*, vol. GE-17, no. 4, pp. 244-249, Oct. 1979.
- [15] I. V. Cherny and V. Y. Raizer, *Passive Microwave Remote Sensing of Oceans*. New York: John Wiley, 1998, pp. 50-64.
- [16] G. S. Bordonskiy, I. B. Vasil'kova, N. N. V. M. Veselov, Y. A. Milititskiy, V. G. Mirovskiy, V. N. Nkitin, V. Y. Raizer, Y. B. Khapin, Y. A. Sharkov, and V. S. Etkin, "Spectral characteristics of the emissivity of foam formations," *Izvestiya, Atmos. Oceanic Phys.*, vol. 14, no. 6, pp. 464-469, 1978.
- [17] L. A. Dombrovskiy and V. Y. Raizer, "Microwave model of a two phase medium at the ocean surface," *Izvestiya, Atmos. Oceanic Phys.*, vol. 28, no. 8, pp. 650-656, 1992.
- [18] A. Camps, M. Vall-Illussera, R. Villarino, N. Reul, B. Chapron, I. Corbella, N. Duffo, F. Torres, J. Miranda, R. Sabia, A. Monerris, R. Rodriguez, "The Emissivity of Foam-Covered Water Surface at L-Band: Theoretical Modeling and Experimental Results From the Frog 2003 Field Experiment," *IEEE Trans. Geosci. Remote Sens.*, vol. 43, no. 5, pp. 925-937, May 2005.